Unconventional Magnetism via Optical Pumping of Interacting Spin Systems

Citation

Published Version

Permanent link

Terms of Use

Share Your Story

Unconventional Magnetism via Optical Pumping of Interacting Spin Systems

Tony E. Lee,[1] Sarang Gopalakrishnan,[2] and Mikhail D. Lukin[2]

[1]*ITAMP, Harvard-Smithsonian Center for Astrophysics, Cambridge, Massachusetts 02138, USA*
[2]*Department of Physics, Harvard University, Cambridge, Massachusetts 02138, USA*
(Received 19 April 2013; published 19 June 2013)

We consider strongly interacting systems of effective spins, subject to dissipative spin-flip processes associated with optical pumping. We predict the existence of novel magnetic phases in the steady state of this system, which emerge due to the competition between coherent and dissipative processes. Specifically, for strongly anisotropic spin-spin interactions, we find ferromagnetic, antiferromagnetic, spin-density-wave, and staggered-*XY* steady states, which are separated by nonequilibrium phase transitions meeting at a Lifshitz point. These transitions are accompanied by quantum correlations, resulting in spin squeezing. Experimental implementations in ultracold atoms and trapped ions are discussed.

Exotic magnetic states play a central role in the physics of quantum many-body systems and have been explored in a wide variety of strongly correlated materials [1]. Realizing and exploring magnetic states has recently emerged as a central goal in ultracold atomic physics [2,3]. Due to highly controllable and tunable interactions, ensembles of ultracold neutral atoms and ions may provide a unique laboratory to study exotic quantum magnetism [2–9]. Among the main obstacles are relatively small energy scales associated with magnetic ordering (e.g., the superexchange scale in the Hubbard model), requiring cooling atomic systems down to very low temperatures [2], and the slow time scales involved in spin thermalization [10–12]. Furthermore, ultracold atoms are fundamentally open, driven quantum systems far from their absolute thermal equilibrium. This motivates the exploration of spin dynamics in the presence of driving and dissipation [13–30].

Recently, a number of schemes involving dissipation to create magnetic phases have been proposed. These typically use engineered reservoirs involving coupling multiple lattice sites [13–15]. At the same time, one expects single-site dissipation such as spontaneous decay to be detrimental to realizing interesting magnetic states, resulting, e.g., in unwanted decoherence. In this Letter, we demonstrate that optical pumping and spontaneous decay can instead *enrich* the phase diagram, resulting in new phases and phase transitions that do not exist in conventional equilibrium systems. Significantly, these novel states can be observed under conditions when the realization of conventional equilibrium states is difficult.

The key idea of this work can be understood by considering the anisotropic spin-1/2 Heisenberg model (i.e., the *XYZ* model), which is governed by the Hamiltonian

$$H = \frac{1}{2d} \sum_{\langle mn \rangle} (J_x \sigma_m^x \sigma_n^x + J_y \sigma_m^y \sigma_n^y + J_z \sigma_m^z \sigma_n^z), \quad (1)$$

where σ_n^x, σ_n^y, σ_n^z are the Pauli matrices for an effective spin n. We assume that the spins are localized on a d-dimensional cubic lattice with nearest-neighbor interactions. In the presence of conventional optical pumping, this Hamiltonian is augmented with a dissipative process that flips the spins down at some rate γ [i.e., it corresponds to the jump operator σ_n^- on every site, where $\sigma_n^\pm = (\sigma_n^x \pm i \sigma_n^y)/2$].

The steady state of this open many-body system is easy to understand in the case of isotropic spin-spin interactions, namely, the *XXZ* model (with either ferromagnetic or antiferromagnetic couplings). For this, the Hamiltonian can be rewritten in the form $H = (1/2d) \sum [2J_x(\sigma_m^+ \sigma_n^- + \sigma_m^- \sigma_n^+) + J_z \sigma_m^z \sigma_n^z]$. This Hamiltonian conserves the total number of spins in the $|\uparrow\rangle$ state and, therefore, does nothing to counteract the spontaneous decay. Thus, the steady state is a trivial dark state with all spins polarized, $|\downarrow\downarrow \cdots \downarrow\rangle\langle\downarrow\downarrow \cdots \downarrow|$, so the *XXZ* model never experiences a phase transition in the presence of dissipation, regardless of J_x and J_z.

However, new types of magnetic order emerge for strongly anisotropic couplings. The crucial role of anisotropy can be understood as follows. Each spin experiences
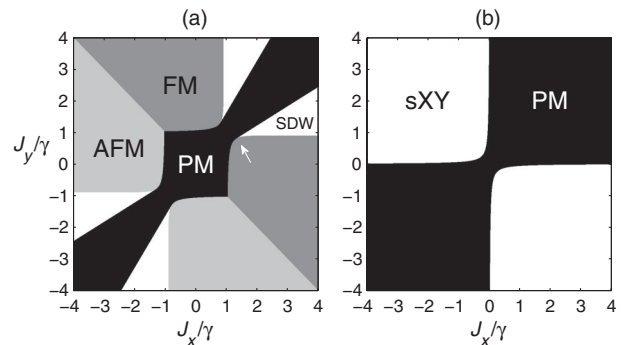

FIG. 1. Mean-field phase diagrams for the dissipative *XYZ* model with (a) $J_z/\gamma = 1$ and (b) $J_z = 0$, showing the different phases: paramagnetic (PM), ferromagnetic (FM), antiferromagnetic (AFM), spin-density-wave (SDW), and staggered-*XY* (sXY). The white arrow points to a Lifshitz point.

an effective magnetic field ($J_x\langle\sigma^x\rangle$, $J_y\langle\sigma^y\rangle$, $J_z\langle\sigma^z\rangle$), which depends on the direction of its neighbors [Fig. 2(a)]. It precesses about this effective field and also decays towards $|\downarrow\rangle$. In order for the spin to point away from $|\downarrow\rangle$ in steady state, its precession must be strong enough to counteract the decay. In the isotropic case, the spin is always parallel to the magnetic field, so there is no precession at all. On the other hand, when the couplings are sufficiently anisotropic (e.g., $J_x \approx -J_y$), the spin is roughly *perpendicular* to the magnetic field, so the precession is strong enough to point the spin away from $|\downarrow\rangle$ [Fig. 2(a)]. This is in sharp contrast to the thermal equilibrium state, in which the spin tries to align with the magnetic field rather than precess about it.

This competition between precessional and dissipative dynamics gives rise to a remarkable phase diagram (Fig. 1), including ferromagnetic and antiferromagnetic phases as well as spin-density-wave and staggered-*XY* phases that do not exist in equilibrium. The spin-density-wave, paramagnetic, and ferromagnetic phases meet at multicritical Lifshitz points, at which the period of the spin-density wave diverges [31]; such Lifshitz points have been seen in equilibrium magnets with long-range interactions [32,33], but generally do not exist in nearest-neighbor spin models. In addition, we find that a continuous symmetry emerges for certain couplings; the spontaneous breaking of this symmetry leads to a phase we call the staggered-*XY* phase. Finally, we find that quantum correlations (as measured by spin squeezing) persist near the phase transitions.

The model described here can be implemented in systems of trapped ions or systems of ultracold atoms with anisotropic superexchange or dipolar interactions. The spin states $|\uparrow\rangle$ and $|\downarrow\rangle$ correspond to two electronic states of the ion or atom. In the case of ions, the spin-spin interaction is obtained through virtual transitions involving motional
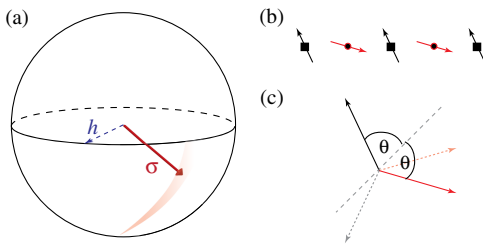

FIG. 2 (color online). (a) Bloch-sphere plot, showing mean-field values of $\langle\vec{\sigma}\rangle$ (solid red arrow) and effective magnetic field (dashed blue arrow) for $J_x/\gamma = -J_y/\gamma = 1$, $J_z = 0$. The vectors are normalized to unit length. [(b) and (c)] sXY phase in the xy plane of the Bloch sphere; (b) one possible stable configuration. Black (pointing upper left) and red arrows (pointing lower right) correspond to sublattices A and B. (c) The A sublattice (black solid arrow) generates a magnetic field (gray dashed arrow) that the B sublattice (red solid arrow) precesses around. Similarly, the B sublattice generates a magnetic field (pink dashed arrow) that the A sublattice precesses around. The angle θ can take any value.

sidebands [4,34,35]. In the case of ultracold atoms, the spin-spin interaction is obtained using a two-photon resonance that excites and deexcites atoms in pairs [36], as explained in the Supplemental Material [37], or using superexchange interactions in p-band optical lattices [38]. In all cases, dissipation can be controllably introduced using optical pumping.

Model.—We now turn to detailed analysis of the phenomena outlined above. The dynamics of the many-body system are given by a master equation for the density matrix ρ,

$$\dot{\rho} = -i[H,\rho] + \gamma\sum_n\left[\sigma_n^-\rho\sigma_n^+ - \frac{1}{2}(\sigma_n^+\sigma_n^-\rho + \rho\sigma_n^+\sigma_n^-)\right].$$

(2)

Equation (2) has a unique steady-state solution [39], and we are interested in whether the steady state exhibits a phase transition as the parameters J_x, J_y, J_z change. Note that the decay is independent for each spin, in contrast with the Dicke model [29,40]. Furthermore, the spins are not in equilibrium with the environmental bath. Thus, in contrast with the spin-boson model [41,42], the steady state is *not* the joint ground state of the system and environment.

The master equation has a Z_2 symmetry (σ_n^x, $\sigma_n^y \rightarrow -\sigma_n^x$, $-\sigma_n^y$), which is spontaneously broken in the ordered phases. In practice, there may also be dephasing noise, leading to dissipative terms in Eq. (2) such as $\sigma_n^z\rho\sigma_n^z$; since the Z_2 symmetry is unaffected by these terms, the phase transitions we describe are robust to dephasing, although the phase boundaries are shifted.

Mean-field theory.—We begin by solving for the steady states of the model Eq. (2) at the level of mean-field theory. We allow the mean field to vary on each site to account for spatially inhomogeneous states [21]. The mean-field equations, which are simply nonlinear Bloch equations, are

$$\frac{d\langle\sigma_n^x\rangle}{dt} = -\frac{\gamma}{2}\langle\sigma_n^x\rangle + \frac{1}{d}\sum_m[J_y\langle\sigma_n^z\rangle\langle\sigma_m^y\rangle - J_z\langle\sigma_n^y\rangle\langle\sigma_m^z\rangle],$$

$$\frac{d\langle\sigma_n^y\rangle}{dt} = -\frac{\gamma}{2}\langle\sigma_n^y\rangle + \frac{1}{d}\sum_m[J_z\langle\sigma_n^x\rangle\langle\sigma_m^z\rangle - J_x\langle\sigma_n^z\rangle\langle\sigma_m^x\rangle],$$

$$\frac{d\langle\sigma_n^z\rangle}{dt} = -\gamma(\langle\sigma_n^z\rangle + 1) + \frac{1}{d}\sum_m[J_x\langle\sigma_n^y\rangle\langle\sigma_m^x\rangle - J_y\langle\sigma_n^x\rangle\langle\sigma_m^y\rangle],$$

(3)

where the sum over m is taken over nearest neighbors of n. (A related model with only dephasing noise was studied in Refs. [43,44]. Another related model with an external field and nonlinear damping was studied using the Landau-Lifshitz-Gilbert equation [45,46].)

Clearly, there is always a fixed-point solution, $\langle\sigma_n^x\rangle = \langle\sigma_n^y\rangle = 0$, $\langle\sigma_n^z\rangle = -1$, in which all the spins are pointing down. We call this the paramagnetic (PM) phase, since it does not break the Z_2 symmetry of Eq. (2). We now consider the linear stability of the PM phase as a function

of J_x, J_y, J_z [47]. We consider d-dimensional perturbations with wave vector $\vec{k} = (k_1, k_2, \ldots, k_d)$ where $k_\ell = 2\pi/a_\ell$ and a_ℓ is an integer. We find that the PM phase is unstable to perturbations of wave vector $\vec{k}$ when

$$\left(\frac{J_x}{d}\sum_{\ell=1}^{d}\cos k_\ell - J_z\right)\left(\frac{J_y}{d}\sum_{\ell=1}^{d}\cos k_\ell - J_z\right) < -\frac{\gamma^2}{16}. \quad (4)$$

This condition is satisfied only when the couplings are sufficiently anisotropic.

When the PM phase is unstable, the system ends up in a time-independent steady state with $\langle\sigma_n^x\rangle$, $\langle\sigma_n^y\rangle \neq 0$, so it breaks the Z_2 symmetry of the master equation. There are four types of ordered phases. (i) A spatially uniform state, which we call the ferromagnetic (FM) phase, resulting from instability of the PM phase to $k_\ell = 0$ for all ℓ. (ii) A spatially modulated state with a period of two lattice sites in all directions; i.e., the system divides into two sublattices. We call this the antiferromagnetic (AFM) phase, and it results from instability to $k_\ell = \pi$ for all ℓ. (iii) A spatially modulated state with a period greater than two lattice sites in at least one direction, which we call the spin-density-wave (SDW) phase. This results from instability to all other k_ℓ. (iv) When $J_z = 0$, there is also a staggered-XY (sXY) phase, resulting from instability to both $k_\ell = 0, \pi$, which is discussed below. The phase diagram is shown in Fig. 1. The transitions from the PM phase are continuous, whereas the FM-AFM transition is discontinuous.

We note two unusual features of this phase diagram. First, along the boundary between the PM and SDW phases, the $\vec{k}$ value at which the instability of the PM occurs approaches 0, meaning that the period of the SDW diverges [Fig. 3(a)]. This line culminates in a multicritical Lifshitz point [31] between the PM, FM, and SDW phases. Lifshitz points occur in magnetic models with competing interactions [32,33] but are not found in
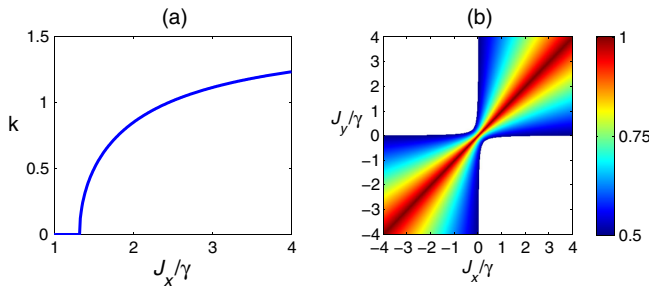

FIG. 3 (color online). (a) Unstable wave vector k along the lower boundary of the PM phase in Fig. 1(a). A Lifshitz point occurs at $J_x/\gamma = 1.32$. For convenience, only one-dimensional wave vectors are shown. (b) Squeezing parameter ζ^2, calculated in the Gaussian approximation for $J_z = 0$. The sXY phase has been whited out, since the Gaussian approximation is not valid there.

equilibrium nearest-neighbor magnets; thus, their existence in nearest-neighbor magnets out of equilibrium indicates that nonequilibrium phase diagrams can be qualitatively richer than those in equilibrium. Lifshitz points show enhanced fluctuation effects relative to conventional critical points [31] and, hence, offer a rich venue for studying quantum fluctuations away from equilibrium.

The second distinctive feature of the phase diagram is that the ordered phase breaks a *continuous* symmetry when $J_z = 0$. In this case, the system divides into two sublattices as in the AFM phase. However, the angle between the two sublattices can take any value. In the specific case of $J_x = -J_y$, the spins on the A and B sublattices are at angles θ and $-\theta$ relative to the $x = y$ line on the Bloch sphere [Fig. 2(b)]. Any value of θ corresponds to a stable configuration, since the sublattices remain perpendicular to each other's magnetic field [Fig. 2(c)]. Upon ordering, this continuous $U(1)$ symmetry between the sublattice spin orientations is spontaneously broken, leading to a phase we call the sXY phase. This phase has vortexlike topological defects around which the relative orientation between A- and B-sublattice spins rotates by 2π.

Comparison with equilibrium.—It is instructive to contrast the above results with the equilibrium case (for $d > 1$). The equilibrium ground state of Eq. (1) is ordered for any J_x, J_y, J_z [48]. The magnetization axis is determined by the strongest of the coupling constants, and the sign of that coupling determines whether the ordering is ferromagnetic or antiferromagnetic. Evidently, the nonequilibrium phase diagram exhibits qualitatively different behavior from this equilibrium case. The qualitative differences between equilibrium and nonequilibrium remain even in the limit $\gamma \to 0$, although the steady state takes an increasingly long time to reach.

Fluctuation effects.—We now turn from mean-field theory to an analysis of fluctuations. Such an analysis was recently performed for driven polariton condensates [49] and suggests that the *static* critical properties (i.e., renormalization-group fixed points) of a driven Markovian system are related to finite-temperature equilibrium critical properties. This would indicate that the dissipative XYZ model discussed here undergoes true phase transitions in two or more dimensions.

We estimate fluctuation effects and squeezing in the Gaussian approximation by mapping the spins to hard-core bosons [48]: $\sigma_n^+ \to b_n^\dagger$, $\sigma_n^z \to 2b_n^\dagger b_n - 1$. This gives a reliable approximation in the PM phase, where $\langle\sigma_n^z\rangle \approx -1$. To Gaussian order (which includes relaxing the hard-core constraint), the resulting Hamiltonian is

$$H = \frac{1}{2d}\left[(J_x + J_y)\sum_{\langle mn\rangle}(b_m^\dagger b_n + b_m b_n^\dagger) + (J_x - J_y)\right.$$
$$\left.\times\sum_{\langle mn\rangle}(b_m^\dagger b_n^\dagger + b_m b_n) - 4dJ_z\sum_n b_n^\dagger b_n\right], \quad (5)$$

and the dissipative terms in the master equation are $\gamma \sum_n [b_n \rho b_n^\dagger - (1/2)(b_n^\dagger b_n \rho + \rho b_n^\dagger b_n)]$. We now use standard Keldysh path-integral techniques [50] to compute the relaxation rate, $\langle \sigma^z \rangle$ and the squeezing. We summarize the results here and provide details in the Supplemental Material [37].

(1) Relaxation rate.—The rate at which the steady state is approached can be read off from the poles of the retarded Green's function. For notational simplicity, we assume $d = 1$ here. In the Gaussian approximation, the lowest pole has complex frequency $-i\gamma/2 \pm 2\sqrt{(J_x \cos k - J_z)(J_y \cos k - J_z)}$. A continuous phase transition occurs when the frequency of this pole approaches zero; this precisely recovers Eq. (4).

(2) Below-threshold fluctuations.—Near the transition, one expects to find nonanalytic behavior in the number of up spins, $\sum_n \langle \sigma_n^z \rangle$. For $J_z = 0$, this scales as $\langle \sigma_z \rangle \sim (\gamma^2 + 16 J_x J_y)^{(d-2)/2}$. The divergence for $d = 1$ renders the Gaussian approximation inconsistent and is related, as we shall show in a future work, to the absence of a phase transition in one dimension (consistent with the polariton-BEC case [49]).

(3) Squeezing.—We find that spin squeezing, a measure of quantum correlations, persists near the transition. It can be calculated using the definition of squeezing for bosons [51]: $\zeta^2 = 1 + 2(\langle b^\dagger b \rangle - |\langle b \rangle|^2) - 2|\langle b^2 \rangle - \langle b \rangle^2|$. For the case of $J_z = 0$, as the phase boundary is approached, $\zeta^2 \rightarrow 1/2$ in the thermodynamic limit for the $k = 0$, π modes, signaling the presence of quantum correlations [Fig. 3(b)].

Comparison with numerics.—We have also simulated the Eq. (2) in one dimension (1D) using the method of quantum trajectories [52]. Although there is presumably no phase transition in 1D, the numerical results already show qualitative features predicted by mean-field theory. For example, when mean-field theory predicts FM, the correlation $\langle \sigma_m^x \sigma_n^x \rangle$ is positive for all distances [Fig. 4(a)]. When there should be AFM, the correlation alternates sign. When there should be SDW, the correlation varies with a wavelength that matches the mean-field value. When there should be sXY, $\langle \sigma_m^x \sigma_n^x \rangle$ and $\langle \sigma_m^y \sigma_n^y \rangle$ are both 0 for odd distances and positive for even distances [Fig. 4(b)]. Furthermore, the gap of the Liouvillian approaches 0 at the boundary of the PM phase, consistent with the Gaussian approximation (see Supplemental Material [37]).

Experimental realization.—The dissipative *XYZ* model can be implemented experimentally using trapped ions. One can use $^{171}\text{Yb}^+$ and let $|\downarrow\rangle$ and $|\uparrow\rangle$ correspond to $^2S_{1/2}|F = 0, m_F = 0\rangle$ and $^2D_{3/2}|F = 2, m_F = 0\rangle$. In the presence of laser beams judiciously detuned from certain motional sidebands, the ions interact via Eq. (1) [4,34,35]. J_x, J_y, J_z can be on the order of 1–5 kHz, and their magnitudes and signs can be varied by changing the laser detunings [4]. By admixing a small component (10^{-4}) of $^2P_{3/2}$ using an off-resonant laser, one broadens the
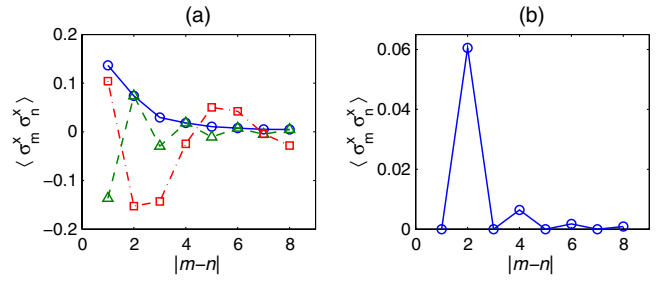

FIG. 4 (color online).   Correlation function $\langle \sigma_m^x \sigma_n^x \rangle$ for 1D chain of 16 spins, from simulating the master equation. (a) $J_z/\gamma = 1$, showing remnant of FM for $J_x/\gamma = 2$, $J_y = 0$ (blue circles, solid line); remnant of AFM for $J_x/\gamma = -2$, $J_y = 0$ (green triangles, dashed line); remnant of SDW for $J_x/\gamma = 4$, $J_y/\gamma = 2$ (red squares, dash-dotted line). The period of the SDW matches the mean-field prediction (5.3 sites). (b) $J_x/\gamma = -J_y/\gamma = 1$, $J_z/\gamma = 0$, showing remnant of sXY phase.

linewidth of $|\uparrow\rangle$ to 2 kHz. (To make this a closed cycle, additional lasers optically pump back into $|\downarrow\rangle$ on a much faster time scale.) Thus, the parameter space shown in Fig. 1 is experimentally achievable. This setup can implement an arbitrary lattice topology for a large number of ions [9,53].

A variety of other realizations of the *XYZ* model are also possible. One approach is to use ultracold atoms coupled via dipole-dipole interactions. The *XYZ* Hamiltonian is implemented by driving a two-photon resonance so that atoms are excited and deexcited in pairs, as explained in the Supplemental Material [37]. This scheme can be realized using Rydberg-dressed atoms [54], Rydberg atoms [36,55,56], or dipolar atoms or molecules [57]. We show explicitly in the Supplemental Material that, for Rydberg-dressed atoms, the parameters needed for the phase transitions (Fig. 1) are experimentally achievable. Finally, one can adapt a recent proposal for realizing *XYZ* models via superexchange in *p*-band optical lattices [38] to include dissipation, by optically pumping the atoms into the p_x orbital via an intermediate excited orbital (e.g., $d_{x^2-y^2}$) that does not decay into the *s* band.

Conclusion.—In summary, we have computed the phase diagram of anisotropic spin models subject to spontaneous decay and shown that these models exhibit phases (SDW and sXY) and phase transitions (Lifshitz point) that are not found in similar equilibrium models. The qualitative differences can be traced to the fact that in equilibrium, spins align with the magnetic field, whereas away from equilibrium, they precess about it. We find that quantum correlations, as measured by squeezing, persist near the dissipative transitions. This work paves the way for future explorations of critical behavior and nonequilibrium fluctuations near the phase transitions we have identified. A particularly intriguing question is how frustrated interactions (due to a triangular lattice) affect the AFM and sXY phases.

[1] E. Dagotto, Rev. Mod. Phys. **66**, 763 (1994).

[2] L.-M. Duan, E. Demler, and M. D. Lukin, Phys. Rev. Lett. **91**, 090402 (2003).

[3] I. Bloch, J. Dalibard, and W. Zwerger, Rev. Mod. Phys. **80**, 885 (2008).

[4] K. Kim, M.-S. Chang, S. Korenblit, R. Islam, E. E. Edwards, J. K. Freericks, G.-D. Lin, L.-M. Duan, and C. Monroe, Nature (London) **465**, 590 (2010).

[5] J. Simon, W. S. Bakr, R. Ma, M. E. Tai, P. M. Preiss, and M. Greiner, Nature (London) **472**, 307 (2011).

[6] S. Gopalakrishnan, B. L. Lev, and P. M. Goldbart, Phys. Rev. Lett. **107**, 277201 (2011).

[7] P. Strack and S. Sachdev, Phys. Rev. Lett. **107**, 277202 (2011).

[8] A. V. Gorshkov, S. R. Manmana, G. Chen, J. Ye, E. Demler, M. D. Lukin, and A. M. Rey, Phys. Rev. Lett. **107**, 115301 (2011).

[9] J. W. Britton, B. C. Sawyer, A. C. Keith, C.-C. J. Wang, J. K. Freericks, H. Uys, M. J. Biercuk, and J. J. Bollinger, Nature (London) **484**, 489 (2012).

[10] B. Capogrosso-Sansone, S. G. Söyler, N. V. Prokof'ev, and B. V. Svistunov, Phys. Rev. A **81**, 053622 (2010).

[11] P. Medley, D. M. Weld, H. Miyake, D. E. Pritchard, and W. Ketterle, Phys. Rev. Lett. **106**, 195301 (2011).

[12] D. C. McKay and B. DeMarco, Rep. Prog. Phys. **74**, 054401 (2011).

[13] S. Diehl, A. Micheli, A. Kantian, B. Kraus, H. P. Büchler, and P. Zoller, Nat. Phys. **4**, 878 (2008).

[14] F. Verstraete, M. M. Wolf, and J. I. Cirac, Nat. Phys. **5**, 633 (2009).

[15] S. Diehl, A. Tomadin, A. Micheli, R. Fazio, and P. Zoller, Phys. Rev. Lett. **105**, 015702 (2010).

[16] J. Kasprzak et al., Nature (London) **443**, 409 (2006).

[17] I. Carusotto and C. Ciuti, Rev. Mod. Phys. **85**, 299 (2013).

[18] E. G. D. Torre, E. Demler, T. Giamarchi, and E. Altman, Nat. Phys. **6**, 806 (2010).

[19] H. Weimer, M. Müller, I. Lesanovsky, P. Zoller, and H. P. Büchler, Nat. Phys. **6**, 382 (2010).

[20] J. Cho, S. Bose, and M. S. Kim, Phys. Rev. Lett. **106**, 020504 (2011).

[21] T. E. Lee, H. Häffner, and M. C. Cross, Phys. Rev. A **84**, 031402 (2011).

[22] T. E. Lee, H. Häffner, and M. C. Cross, Phys. Rev. Lett. **108**, 023602 (2012).

[23] C. Ates, B. Olmos, J. P. Garrahan, and I. Lesanovsky, Phys. Rev. A **85**, 043620 (2012).

[24] B. Olmos, I. Lesanovsky, and J. P. Garrahan, Phys. Rev. Lett. **109**, 020403 (2012).

[25] F. Nissen, S. Schmidt, M. Biondi, G. Blatter, H. E. Türeci, and J. Keeling, Phys. Rev. Lett. **108**, 233603 (2012).

[26] E. M. Kessler, G. Giedke, A. Imamoglu, S. F. Yelin, M. D. Lukin, and J. I. Cirac, Phys. Rev. A **86**, 012116 (2012).

[27] M. Höning, M. Moos, and M. Fleischhauer, Phys. Rev. A **86**, 013606 (2012).

[28] M. Foss-Feig, K. R. A. Hazzard, J. J. Bollinger, and A. M. Rey, Phys. Rev. A **87**, 042101 (2013).

[29] E. G. D. Torre, S. Diehl, M. D. Lukin, S. Sachdev, and P. Strack, Phys. Rev. A **87**, 023831 (2013).

[30] C. Carr, R. Ritter, C. S. Adams, and K. J. Weatherill, arXiv:1302.6621.

[31] R. M. Hornreich, M. Luban, and S. Shtrikman, Phys. Rev. Lett. **35**, 1678 (1975).

[32] M. Grousson, G. Tarjus, and P. Viot, Phys. Rev. E **62**, 7781 (2000).

[33] R. Jamei, S. Kivelson, and B. Spivak, Phys. Rev. Lett. **94**, 056805 (2005).

[34] K. Mølmer and A. Sørensen, Phys. Rev. Lett. **82**, 1835 (1999).

[35] D. Porras and J. I. Cirac, Phys. Rev. Lett. **92**, 207901 (2004).

[36] I. Bouchoule and K. Mølmer, Phys. Rev. A **65**, 041803 (2002).

[37] See the Supplemental Material at http://link.aps.org/supplemental/10.1103/PhysRevLett.110.257204 for details on experimental implementation and Gaussian fluctuations.

[38] F. Pinheiro, G. M. Bruun, J. P. Martikainen, and J. Larson, arXiv:1304.3178.

[39] S. G. Schirmer and X. Wang, Phys. Rev. A **81**, 062306 (2010).

[40] D. Nagy, G. Szirmai, and P. Domokos, Phys. Rev. A **84**, 043637 (2011).

[41] A. J. Leggett, S. Chakravarty, A. T. Dorsey, M. P. A. Fisher, A. Garg, and W. Zwerger, Rev. Mod. Phys. **59**, 1 (1987).

[42] P. Werner, K. Völker, M. Troyer, and S. Chakravarty, Phys. Rev. Lett. **94**, 047201 (2005).

[43] A. Vardi and J. R. Anglin, Phys. Rev. Lett. **86**, 568 (2001).

[44] J. R. Anglin and A. Vardi, Phys. Rev. A **64**, 013605 (2001).

[45] T. Gilbert, IEEE Trans. Magn. **40**, 3443 (2004).

[46] M. Lakshmanan, Phil. Trans. R. Soc. A **369**, 1280 (2011).

[47] M. C. Cross and P. C. Hohenberg, Rev. Mod. Phys. **65**, 851 (1993).

[48] S. Sachdev, Quantum Phase Transitions (Wiley Online Library, New York, 2007).

[49] L. M. Sieberer, S. D. Huber, E. Altman, and S. Diehl, Phys. Rev. Lett. **110**, 195301 (2013).

[50] A. Kamenev and A. Levchenko, Adv. Phys. **58**, 197 (2009).

[51] J. Ma, X. Wang, C. Sun, and F. Nori, Phys. Rep. **509**, 89 (2011).

[52] J. Dalibard, Y. Castin, and K. Mølmer, Phys. Rev. Lett. **68**, 580 (1992).

[53] S. Korenblit, D. Kafri, W. C. Campbell, R. Islam, E. E. Edwards, Z.-X. Gong, G.-D. Lin, L.-M. Duan, J. Kim, K. Kim, and C. Monroe, New J. Phys. **14**, 095024 (2012).

[54] N. Henkel, R. Nath, and T. Pohl, Phys. Rev. Lett. **104**, 195302 (2010).

[55] M. D. Lukin, M. Fleischhauer, R. Cote, L. M. Duan, D. Jaksch, J. I. Cirac, and P. Zoller, Phys. Rev. Lett. **87**, 037901 (2001).

[56] M. Saffman, T. G. Walker, and K. Mølmer, Rev. Mod. Phys. **82**, 2313 (2010).

[57] T. Lahaye, C. Menotti, L. Santos, M. Lewenstein, and T. Pfau, Rep. Prog. Phys. **72**, 126401 (2009).